scientific reports

Check for updates

OPEN

A autophagy related gene signature to predict the prognosis of pancreatic carcinoma and tumor immune microenvironment evaluation

Xujie Wang, Xiaoyi Wang & Bicheng Ying✉

Pancreatic adenocarcinoma (PAAD) has a poor prognosis and responds poorly to immunotherapy. Growing evidence indicates that autophagy promotes tumor progression, and autophagy-related genes (ARGs) have been established as prognostic markers in various cancers. Based on consensus clustering of ARGs, 177 PAAD cases were classified into two subtypes, with cluster B exhibiting weaker anti-tumor immunity. Using univariate COX and Least absolute shrinkage and selection operator (LASSO) regression, 13 ARGs were identified to construct a prognostic model. A risk score formula was developed and validated using the GSE183795 dataset. Patients were divided into high- and low-risk groups, with the high-risk group associated with poorer survival. The model showed strong predictive accuracy, with time-dependent area under the curve (AUC) values ranging from 0.762 to 0.848 in the training cohort and 0.658 to 0.714 in the validation cohort. Further analysis revealed that high-risk patients had suppressed immunity but increased sensitivity to certain chemotherapy drugs. Additionally, high tumor mutational burden (TMB) and RNA stemness score (RNAss) were correlated with worse prognosis in high-risk patients. This ARG-based model effectively predicts PAAD outcomes and may guide clinical treatment strategies.

Keywords Pancreatic carcinoma, Autophagy, Immune infiltration, Tumor mutation, Drug-Sensitive, Prognostic value

Abbreviations

PAAD	Pancreatic adenocarcinoma
PC	Pancreatic carcinoma / Pancreatic cancer
HADB	Human Autophagy Database
THANATOS	http://thanatos.biocuckoo.org
HAMdb	http://hamdb.scbdd.com
ARGs	Autophagy-related genes
DEARGs	ARGs with differentially expressed genes
DEGs	Differentially expressed genes

Pancreatic carcinoma (PC) is one of the deadliest malignant cancers of the digestive tract in the world, and its 5-year overall survival (OS) rate is less than 10%[1]. PAAD may replace breast cancer, colorectal and prostate cancer as the second leading source of cancer-related death[2]. The patients with PAAD were classified into I ~ IV grade according to Computed Tomography (CT) images. However, when a tumor is found, it has usually metastasized and spread, making it extremely difficult to remove[3]. Although adjuvant therapy including radiation therapy, chemical drug therapy and molecular targeted drug therapy have made progress, the survival rate of sufferers with PAAD is still very low[4]. However, due to the complexity and heterogeneity among tumor cells, the clinical results are not satisfactory. Thus, it is imperative to carry out personalized treatment. In addition, the discovery of applicable prognostic markers may contribute to the development of individualized therapeutics.

Autophagy plays an important role in maintaining the dynamic balance of cells and organisms. And participate in biological systems that degrade proteins and cellular components, so that cells can be dynamically

Ninghai First Hospital, Ninghai, Ningbo, China. ✉email: 1106795815@qq.com

balanced and energy balance can be maintained[5]. Some scholars had found that the disorder of autophagy is the cause of a wide range of pathological diseases, including malignant tumors[6,7] and cardiovascular diseases[8], neurodegenerative diseases[9], metabolic diseases[10], lung diseases[11], kidney diseases[12], infectious diseases[13], musculoskeletal diseases[14] and eye diseases. In malignant tumors, autophagy plays a dual character by inhibiting cancer initiation and supporting cancer progression[15]. In detail, autophagy plays a dynamic role in tumor inhibition or promotion in different backgrounds and stages of malignant tumors development. In the initial stage of tumor, autophagy can prevent the occurrence of tumor and inhibit the development of tumor. It is regulated by a way of survival and quality control mechanism. As long as the tumor develops to an advanced stage and was affected by environmental stress, autophagy helps the survival and growth of established tumors through a dynamic degradation and circulatory system, and promotes malignant tumors invasiveness by promoting metastasis[16]. Sui et al. proved that autophagy is a possible biomarker in anticancer treatment, and drug tolerance and disease advancement are closely related to autophagy[17]. At present, ARGs have been constructed to forecast the prognosis of a variety of malignant cancer, such as colon cancer[18], lung adenocarcinoma[19] and breast invasive carcinoma[20]. Yet, the correlation between autophagy and PAAD is not clear so far.

The research used multiple public databases such as The Cancer Genome Atlas Dataset (TCGA), Genotype-Tissue Expression (GETx), Gene Expression Omnibus (GEO), Human Protein Atlas (HPA). A predictive model consisting of 13 ARGs was constructed by univariate COX and LASSO analysis, and its accuracy and validity are verified. The single sample gene set enrichment analysis (ssGSEA), Immunological characteristics, Immunosuppressive molecule, Major histocompatibility vomplex (MHC) molecular and stimulator genes analysis and prediction of IC50 have guiding significance for immunological therapy. The high-risk population chort showed a high RNAss, which means that they have the ability to disease progression, distant metastasis and drug tolerance. We consider that this research will guide therapy options and offer some new study directions for enhancing autophagy against PC.

Materials and methods

RNA-seq data from public databases

Public PAAD RNA sequencing materials and corresponding clinicopathological data were derived from TCGA and GEO dataset. The RNA-seq datasets of pancreas were downloaded from the GTEx portal. We extracted 177 patients with PAAD from TCGA database and PC with complete clinicopathological materials as training cohort. Then the Fragments per kilobase of transcript per million fragments mapped data (FPKM) gene expression matrix data were processed and turned into Transcripts per kilobase million values (TPM) data. In addition, the RNA-seq data and survival data of 139 PC patients in the GSE183795 set were used as external validation queues. In addition, the set of genes related to human autophagy-dedicated was extracted from the human autophagy database.

Selection of ARGs and ARGs related to prognosis

A total of 232 ARGs related to human autophagy-dedicated were collected from multiple public database (HADB, THANATOS, HAMdb) and stored in Supplementary Table 1. Then, according to the R "LIMMA" package, the differentially expressed genes (DEGs) between normal and tumor samples in the training queue were screened. The filtering criteria are $|\log_2 FC| > 1$ and $p < 0.05$. Finally, DEGs related to autophagy were obtained. The STRING database is used to list the network diagram of protein-protein interaction (PPI) between DEARGs. The PPI results are then presented through Cytoscape (v3.8.0). In addition, GO and KEGG analysis revealed the functions or related pathways of these DEGs[21]. Next univariate COX analysis ($p < 0.05$) was used to select the ARGs related to prognosis, then draw the related network diagram and intersection Venn diagram by R software. And the KM survival curve is drawn for DEARGs.

Subtype cluster recognition

The DEARGs of PC sufferers in TCGA-PAAD cohort was analyzed by subtype cluster analysis. The cohort was divided into different subtypes according to R "ConensusClusterPlus". Specifically, according to the 28 autophagy-related's prognostic genes (ARPGs), we further divided the 177 PC samples into two different clusters by unsupervised cluster analysis. 66 cases were divided into cluster A and 111 cases were divided into cluster B. In this study, the OS, progression-free survival (PFS), disease-free survival (DFS) and disease-specific survival (DSS) of patients with PC were analyzed and visualized. The heatmap is used to show the clinicopathological differences between different subtypes (such as tumor stage, histology). In addition, the pathway of functional enrichment among different subtypes was explored by Gene Set Variation Analysis (GSVA). Then ssGSEA analysis was used to study the differences of tumor infiltrating immune cells and immune function among PC subtypes. The tumor microenvironment (TME) scores among different subtypes were evaluated by "ggpubr" package.

Establishment and validation of the Autophagy-Related risk signature

On the basis of univariate COX analysis to extract prognostic parameters, LASSO-COX regression analysis was used to determine the core genes, so as to construct the corresponding prognostic risk characteristics and draw risk model. Then, according to the median risk score of sufferers in the TCGA-PAAD cohort, PC sufferers were divided into two different high- and low-risk groups. KM analysis was used to compare the prognostic correlation between high and low risk groups. Then the correlation diagram of risk factors between the two groups is drawn to show the differences between the two groups. Principal component analysis (PCA) is a technique that simplifies the analysis of two sets of data and uses the "rgl" R package for 3D visualization. In addition, in order to increase the accuracy and reliability of the model, we validate the GSE183795 queue as an external verification.

The relationship between risk characteristics and clinicopathological data
In order to reveal the potential clinical significance of the risk model, the correlation between risk score and clinicopathological features was analyzed in the TCGA and GSE183795 set.

The construction of nomogram and its correction curve
Univariate COX and multivariate COX were used to analyze whether the risk score and clinicopathological features were independent risk factors. The receiver operating characteristic (ROC) curves were generated by the timeROC package. The prognostic efficiency of the model was measured by the AUC. ROC curve was established to compare the effects of different factors on prognosis. Finally, the nomogram and correction curve of OS for 2-, 3- and 4-years are drawn.

Prognostic analysis and enrichment analysis of different risk groups
Patients with PC were divided into different clinical subgroups according to tumor stage (T1-2, T3-4, N0-N1, M0-M1), tumor stage (stage I-II, III-IV), histology (G1-2, G3-4) (Supplementary Table 2). KM survival analysis was used to further evaluate whether there were differences in high and low risk cohorts among different clinical subtypes. The differences and functional approaches between high and low risk cohorts are discussed by using GSVA and GSEA methods. The enrichment analysis of differential genes in high and low risk groups was analyzed by GO and KEGG.

Immune-Related analysis
In this study, a variety of immune infiltration algorithms were used to explore the correlation of cancer infiltrating immune cells in two different risk groups. The relation between 13 ARGs and immune cell infiltration was analyzed by "CIBERSORT". The activation of immunosuppressive molecules, MHC molecules, immune checkpoints and stimulating factor genes among different risk groups were evaluated.

DNA methylation analysis
MEXPRESS (https://mexpress.be/) is a database that visualizes the relationship between patient clinical information-methylation-expression in the TCGA database. The study utilized the MEXPUSS web server to estimate and visualize DNA methylation of 13 ARPGs in the TCGA cancer dataset.

Copy number variations and genetic mutation
Sort out the copy number variation (CNV) and somatic mutation information in TCGA-PAAD data. The waterfall diagram is used to show the mutation between high and low risk groups.

Evaluation of immunohistochemical staining
The corresponding immunohistochemical (IHC) staining results were obtained from the human protein atlas database to evaluate the protein expression between normal pancreatic and pancreatic cancer tissues.

Drug-Sensitive and cancer stem cell correlation analysis
tumor immune dysfunction and exclusion (TIDE) score will better help oncologists to select pancreatic cancer patients who are more suitable for immunosuppressive therapy. The online Genomics of Drug Sensitivity database was used for analysis. And the sensitivity of commonly used chemotherapy drugs in sufferers with PC was analyzed, and the outcomes were calculated and expressed by IC50. Finally, the relation between risk score and RNAss is analyzed and visualized.

Statistical analysis
In this study, the bioinformatics data were analyzed by R software (version 4.2.1). According to the different data types, the datas were analyzed by student's t-test and Wilcoxon non-parametric test. Correlation analysis using Spearman method. $P < 0.05$ was regarded statistically significant.

Results
Research flow chart
The flow chart of the research was shown in Fig. 1.

Difference analysis and enrichment analysis of ARGS
Get the DEARGs from the TCGA-PAAD queue according to the filtering criteria (|Log2 FC| >1, p-value < 0.05). The results show that a total of 73 ARGs were obtained. Compared with normal pancreatic tissue, 39 ARGs were up-regulated and 34 ARGs were down-regulated (Figure.2 A). The results of PPI analysis were obtained by screening criteria with high confidence (0.7), and the functional association network of DEARGs was drawn (Figure.2B). In addition, taking the cutoff value > 0.4 as the standard, the correlation coefficient between DEARGs were calculated and the graph is drawn (Figure.2 C). And most ARGs have positive control relation except for negative correlation among EIF4EBP1, TP53INP2, ERN1, EIF2AK3, MAPK8IP1. Then, in order to better understand the potential biological functions of these DEARGs, we carried out GO analysis. And The results show that the GO terms of ARGs were "regulation of autophagy, autophagosome organization and macroautophagy" in BP, "autophagosome and phagocytic vesicle" in CC, and "heat shock protein binding and biquitin protein ligase binding" in MF. The results of enrichment analysis showed that there was a close relationship between differential genes and autophagy (Figure.2D). KEGG analysis shows that the main enrichment of ARGs are multiple signal pathways, such as "mTOR, FoxO and PI3K-Akt signaling pathway", "Pancreatic cancer", "Autophagy-animal", "Apoptosis and other pathways" (Figure.2E).

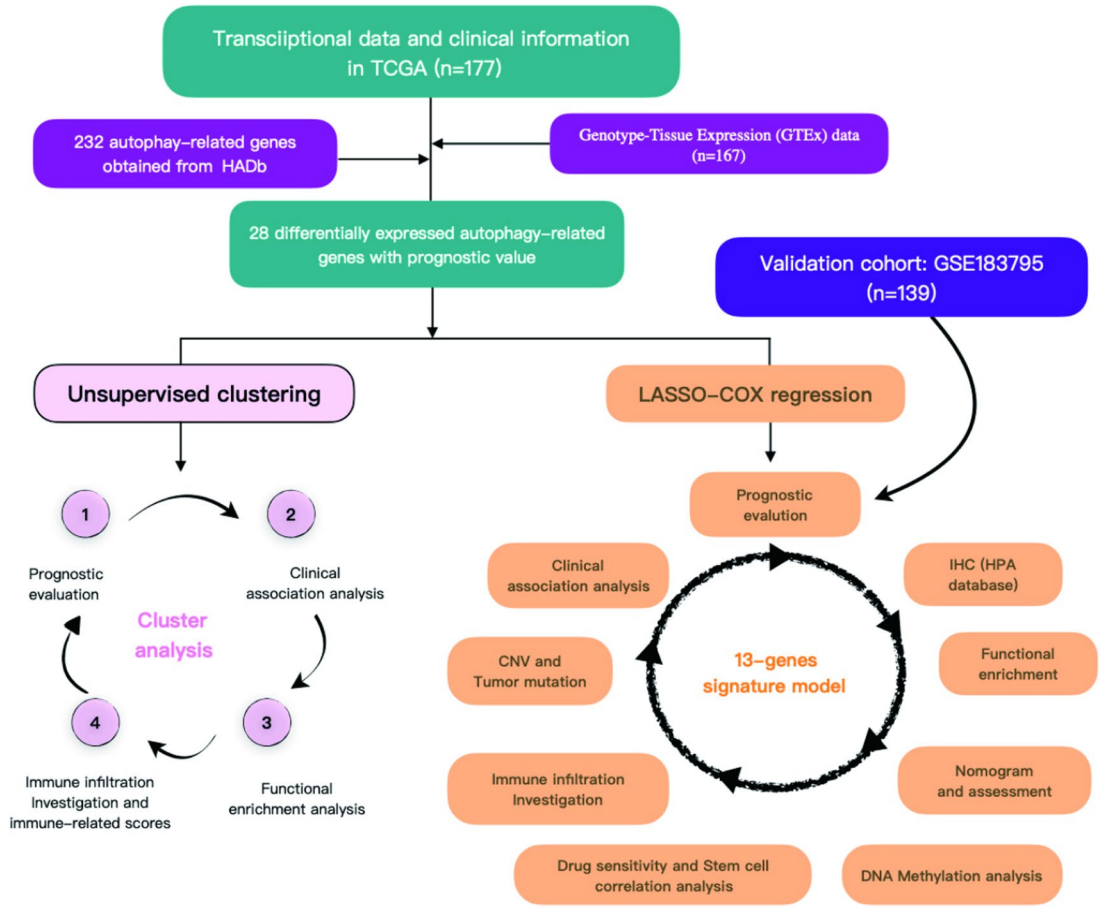


Fig. 1. shows the research flow.

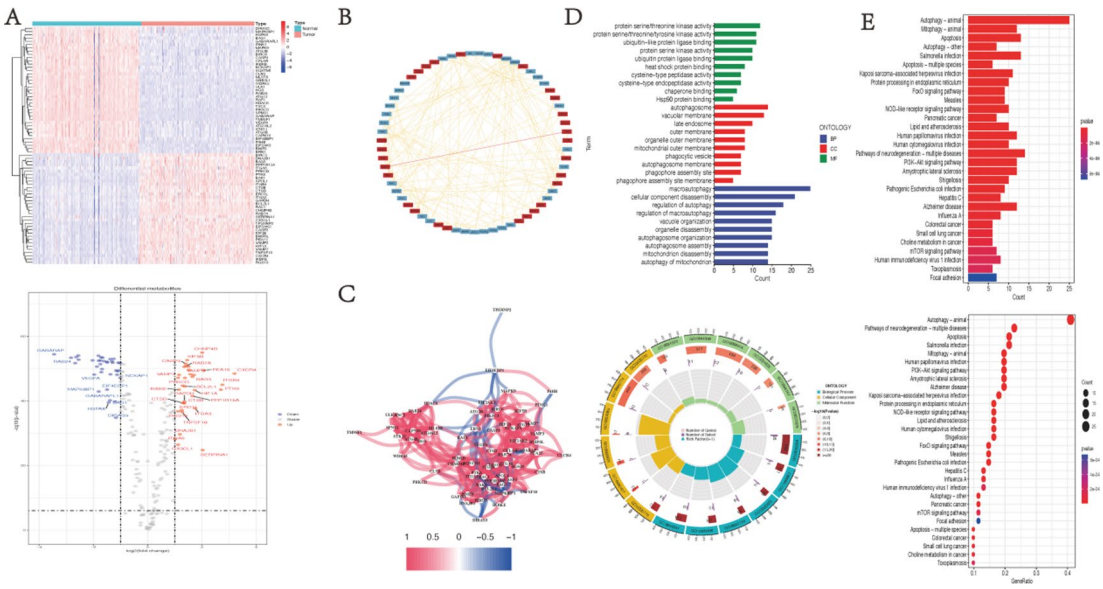


Fig. 2. Differential expression and enrichment analysis of ARGs. (**A**) Heat map and volcano map of DEARGs in TCGA-PAAD set (Screening criteria |log2FC| >1, p-value < 0.05). (**B**) PPI network diagram of DEARGs. (**C**) The regulatory diagram of DEARGs. (**D**) GO analysis of DEARGs. (**E**) KEGG analysis of DEARGs.

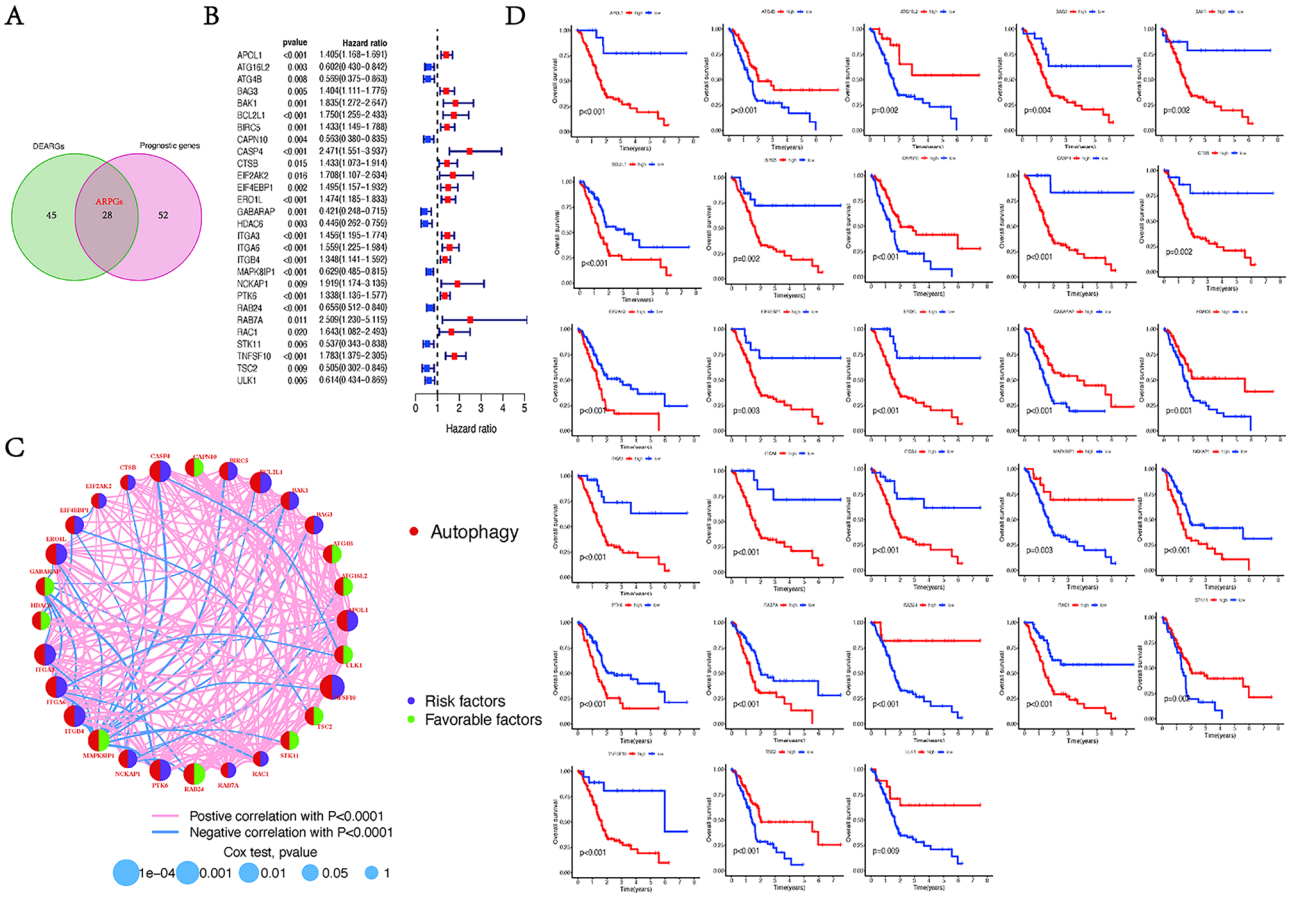


Fig. 3. Identification of ARGs related to prognosis. (**A**) Venn diagram of DEARGs and prognosis-related genes. (**B**) Through univariate COX analysis, 28 ARPGs with different risk ratios were shown by forest map (p-value < 0.05). (**C**) The interaction network diagram of ARPGs. (**D**) The high and low expression OS curves of 28 ARPGs.

Establishment of ARGs related to prognosis

On the basis of 73 DEARGs, the ARPGs was determined by univariate COX analysis ($p < 0.05$). Finally, 28 ARPGs were obtained (Figure.3 A). And a forest map was drawn to show 28 ARPGs results (Figure.3B). Specifically, except for ATG16L2, ATG4B, CAPN10, GABARAP, HDAC6, MAPK8IP1, RAB24, STK11, TSC2 and ULK1, other ARPGs were considered to be a risk factor for PC sufferers in the TCGA-PAAD cohort (Supplementary Table 3). Then the network diagram between them was drawn (Figure.3 C). In addition, we demonstrated the effect of ARPGs expression on OS in patients with PC by KM survival analysis (Figure.3D).

Unsupervised clustering analysis of PC subtypes based on 28 arpgs

According to the 28 ARPGs, we further divided the PC samples (TCGA-PAAD set) into two different clusters by unsupervised cluster analysis. Specifically, 66 cases were divided into cluster A and 111 cases were divided into cluster B (Figure.4 A). Through the analysis of several different time points between the two clusters (such as OS, PFS, DFS and DSS), we found that there were significant differences between them, and the prognosis of patients with cluster B was worse than that of patients with cluster A (Figure.4B). Whereafter, the internal relationship between the two subgroups of PC and clinicopathological data was analyzed. Figure.4 C shows that the patients in cluster B are closely related to the high expression of ARPGs and poor clinicopathological parameters (such as N stage, tumor stage and histology), which also confirms that the prognosis of cluster B is worse. Then we analyzed the differences in functional pathway and immune function between the two clusters in two different ways (GSVA and ssGSEA analyses). Through GSVA analyses method, it was found that compared with cluster A, the main KEGG pathways of cluster B included "cell cycle", "DNA replication", "tumor-related pathways (such as bladder and thyroid)", "multiple signal pathways (such as Notch and p53 signal pathway)", and "various metabolism including glutamic acid, pyrimidine metabolism, glycerolipid metabolism as well as glycolysis gluconeogenesis". It is suggested that cluster B may be closely related to the occurrence and evolution of PC (Figure.4D). Furthermore, the differences between the two clusters (cluster A and B) were analyzed, and the results were analyzed by GO and KEGG analysis, and the first 20 rich terms were shown respectively (Figure.4E-4 F). In addition, the immune infiltrating scores were calculated based on the ssGSEA algorithm, and it was found that several immune cells (such as B cells, CD8 + T cells, mast cells, neutrophils, NK cells, pDCs,

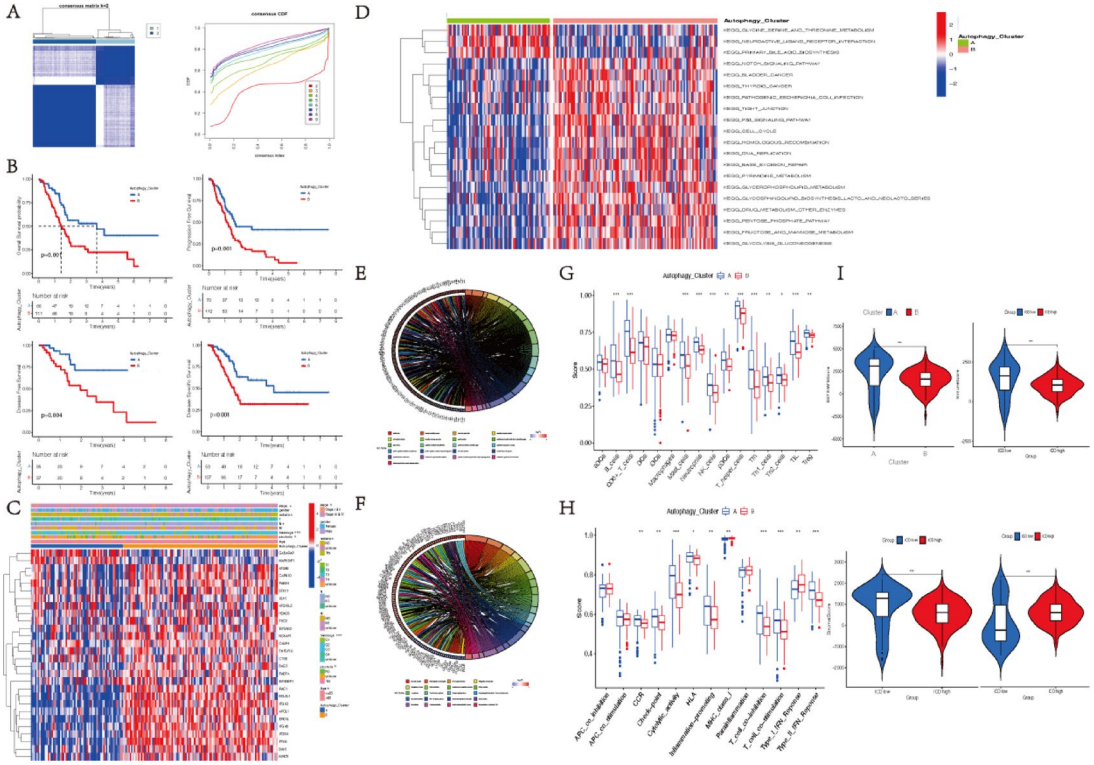


Fig. 4. Unsupervised clustering analysis of ARPGs in the TCGA-PAAD queue. (**A**) Based on unsupervised cluster analysis, all sufferers with pancreatic cancer were divided into two different subtypes (k = 2). (**B**) OS, PFS, DFS and DSS curves of two different subtypes were analyzed. (**C**) The heat map of the relationship between clinicopathological data and PC subgroups. (**D**) Based on the GSVA algorithm, the KEGG analysis in two PC clusters is revealed. (**E**-**F**) chordal diagram of GO and KEGG of DEGs between cluster A and B ($|\log2FC| > 1$, $p < 0.05$). (**G**) The difference of infiltrating immune cells between the two clusters. (**H**) The difference of immune-related function among different clusters. (**I**) Score of immune microenvironment between two clusters.

TIL) had higher permeability levels in cluster A (Figure.4G). Similarly, most immunological functions like checkpoint, human leukocyte antigen, inflammation promotion showed higher scores in cluster A, while Type I IFN Response and MHC class I mainly showed higher scores in cluster B (Figure.4 H). Through the analysis of TME, the results show that cluster B is lower than cluster A in terms of stromal, immune, and estimate scores (Figure.4I). It is well known that the tumor immune microenvironment is closely related to the occurrence and development of tumors and the response to immunotherapy. Therefore, the differences of immune cell infiltration and immune function among different PC subtypes may be the key factors to determine the effect and prognosis of PC immunotherapy.

Establishment and verification of correlation analysis between Autophagy-Related risk signals and clinicopathological parameters

First of all, for 28 ARPGs, the risk model is established by LASSO Cox regression analysis (Figure.S1). Then a risk profile consisting of 13 ARPGs is obtained. The specific formula is as follows: Risk Score = EIF4EBP1×0.182 – HDAC6×0.265 – GABARAP×0.368 + CASP4×0.310 – ATG16L2×0.053 + BCL2L1×0.158 + BAG3×0.032 – ATG4B×0.819 + TNFSF10×0.319 + PTK6×0.094 + ITGA3×0.180 + BIRC5×0.003 + BAK1×0.009 (Supplementary Table 4). The PC sufferers in the train queue were divided into two different risk groups (88 at high risk and 89 at low risk) according to the median risk score. KM survival analysis showed that OS was worse in high-risk group than in low-risk group (Figure.5 A). In addition, similar outcomes were further confirmed in external data sets, with the OS of high-risk group in the GSE183795 cohort even worse (Figure.5B). Then it describes the differences of risk score distribution, survival status and risk gene expression patterns among different risk groups in each cohort (Figure.5 C-5D). Incidentally, we performed immunohistochemical analysis of these ARPGs in normal pancreatic tissue and pancreatic cancer sample, with the exception of GABARAP. From the HPA database analysis, the results can well proved their expression patterns at the protein level (Figure.S2). In addition, we performed t-Distributed Stochastic Neighbor Embedding (t-SNE) and 3D-PCA analysis on the prognostic model (Figure.5E-5 F). The results show that our model can effectively distinguish between high and low risk groups.

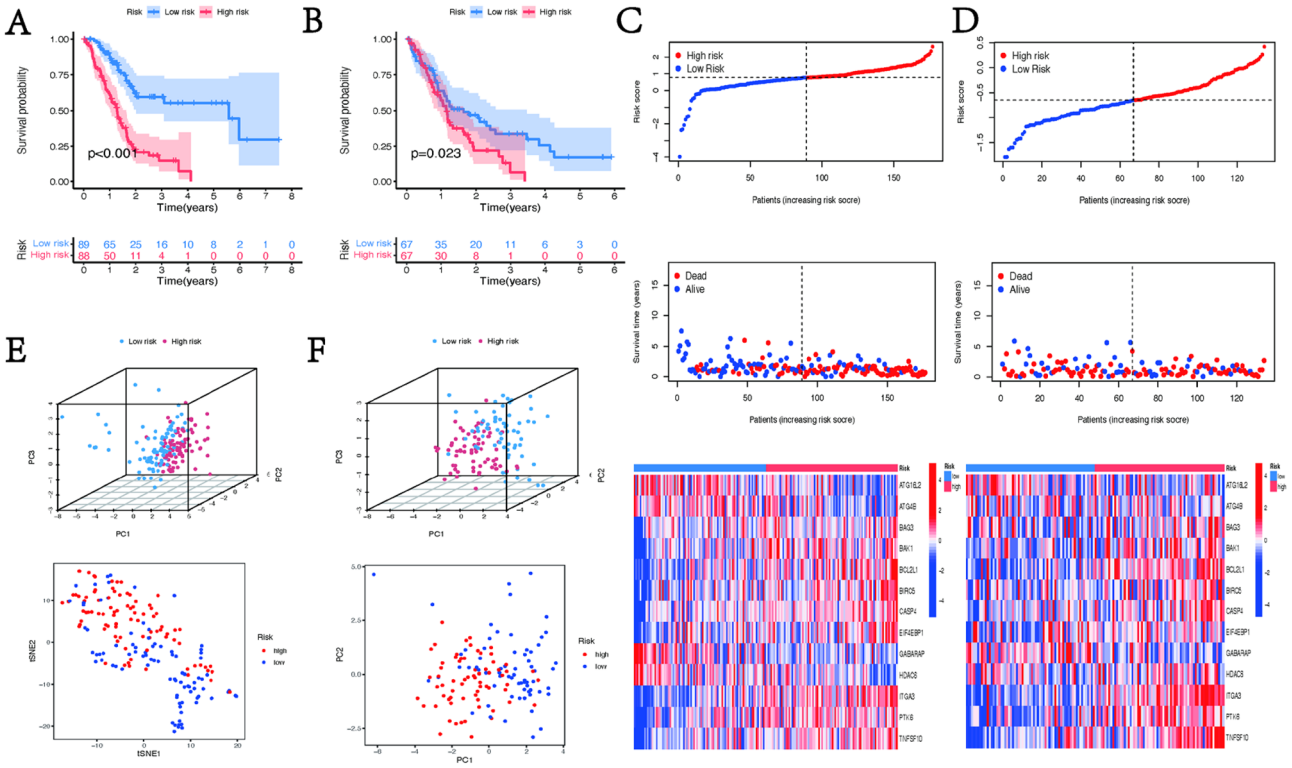


Fig. 5. Development and corroboration of autophagy-related risk model. (**A**-**B**) The OS of the high-risk and low-risk groups in TCGA-PAAD and GSE183795 cohort. (**C**-**D**) risk heatmap in TCGA-PAAD and GSE183795 queue. (**E**-**F**) 3D-PCA and t-SNE analyses between distinct risk groups in the TCGA-PAAD and GSE183795 queue.

Clinicopathological features correlation analysis

Furthermore, in order to study the prognostic value of our signature in pancreatic cancer sufferers with distinct clinicopathological parameters, we explored the relationship between risk groups and clinicopathological data. As shown in Figure.6 A, the high-risk score was significantly associated with tumor stage (Stage III&IV), T stage (T2-3) and histology (G3). At the same time, there was also a significant correlation between risk scores and PC subtypes. And cluster B is more related to risk score than cluster A (Figure.6B). Subsequently, we use Sankey diagram to describe the linear relationship among cluster, risk group and patient's status (Figure.6 C). Additionally, we also compared the OS of high and low risk groups with different clinicopathological parameters (Figure.S3). The relationship between risk score and clinical characteristics in the GSE183795 cohort was analyzed, as shown in Figure.S4. In addition, the correlation between 13 genes and risk score was analyzed in the training cohorts (Figure.6D). In summary, these results show that the 13 genes (including risk characteristics) were significantly correlated with clinicopathological parameters, which highlights the good predictive ability of our results and is expected to be used as a potential prognostic indicator for sufferers with PC.

Nomogram construction and risk model assessment

Furthermore, univariate COX and multivariate COX analysis were used to evaluate the independent predictive effect of risk score and clinicopathological parameters on prognosis. Univariate COX showed that risk score, age, histology, tumor stage were risk factors for prognosis (Figure.7 A). Additionally, multivariate COX further confirmed that the risk score ($p < 0.001$, HR = 4.237, 95% CI: 2.836 – 6.331) and N stage ($p = 0.023$, HR = 1.923, 95% CI: 1.097 – 3.371) were independent hazard factors (Figure.7B). In addition, based on the above results, we constructed a nomogram to forecas the incidence of 2-, 3-, and 4-year OS in sufferers with PC (Figure.7 C). And through the calibration curve, we verify that our nomogram has good consistency and accuracy in predicting OS (Figure.7D). Meanwhile, we performed ROC curve analysis to evaluate the sensitivity and specificity of the model in predicting prognosis. And the area under the ROC curve (AUC) is calculated. The results show that the 2-, 3- and 4-year AUCs of the training cohort are 0.762, 0.806 and 0.848 respectively, and the 2-year, 3-year and 4-year AUC of the verification cohort are 0.658, 0.723 and 0.714 respectively, indicating that our prediction model has good prediction performance (Figure.7E-7 F). In addition, we constructed a 3-year ROC for eight clinicopathological parameters and model parameters, and the results showed that the model was more predictable in TCGA-PAAD cohort (Figure.7G). Decision curve analysis (DCA) results show that our model has more advantages (Figure.7 H).

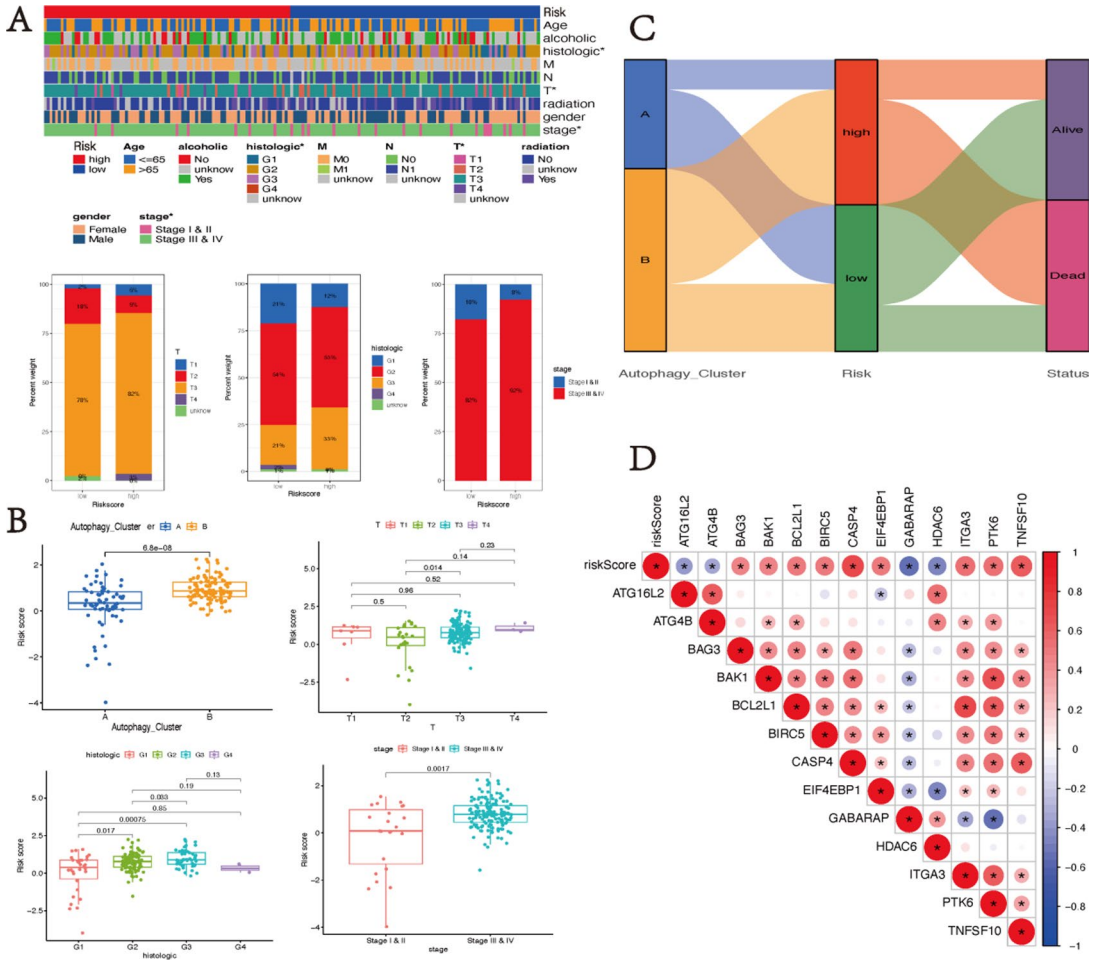


Fig. 6. Clinical characteristics of the risk signature. (**A**) Heatmap of clinical features and risk scores in the training set. The percentage of T stage, histology, tumor stage and the correlation among distinct risk groups. (**B**) Boxplots in the TCGA-PAAD queue with differences in risk scores between different subtypes and different clinicopathological parameters. (**C**) The Sankey diagram shows the linear relationship between the three variables. (**D**) Correlation between 13 genes and risk score.

Enrichment analysis of autophagy-associated risk signature

In order to explore the potential differences in biological processes and functional pathways among different risk groups in the training cohort, we conducted an individual survey by GSVA and GSEA analysis, respectively. First of all, the results of GSVA showed that the significantly rich terms in GO were "negative regulation of apoptotic signaling pathway", "Purine nucleic acid metabolic process", "Deoxyribonucleic acid metabolism process" and "Negative regulation of protein degradation" in BP, "Laminin binding" and "Cadherin binding" in MF, and "Kinetic microtubule" in CC. Moreover, several noteworthy KEGG pathways like "cancer-associated (like Pancreatic cancer, Thyroid carcinoma, bladder cancer) pathways", "cell cycle", "P53 signal pathway", "various metabolism pathways including Amino sugar and nucleotide glucose metabolism", "other enzymes in drug metabolism", "Glycolysis gluconeogenesis" and "Pentose phosphate pathway" were significantly concentrated in patients with PC (Figure.8 A). Whereafter, the above biological annotations were verified by GSEA analysis. The results showed that the KEGG pathways in high risk sufferers were mainly concentrated in "cell cycle", "pathways in cancer", "P53 signal pathway" and "pyrimidine metabolism", whereas "neuroactivity ligand receptor interaction", "ribosome", as well as "intestinal immune network for the production of immunoglobulin" were mainly concentrated in low-risk people (Figure.8B). Subsequently, GO analysis showed that the most common terms related to high risk scores were "mitotic nuclear division", "nuclear chromosome separation", and "sister chromosome separation", while "B cell receptor signaling pathway", "immunoglobulin production", "T cell receptor complex", "Phagocytic recognition" were associated with low risk patients (Figure.8 C). In addition, a total of 100 DEGs were screened out between the high and low risk groups using the filter criteria of $|\log2FC| > 1$ and $p < 0.05$. Meanwhile, these DEGs were analyzed by GO and KEGG (Figure.8D).

Explore the characteristics of immunity

Immune landscape based on many different immune algorithms. The results showed that there were significant differences in the infiltration of immune cells among different risk groups. The infiltration level of immune cells

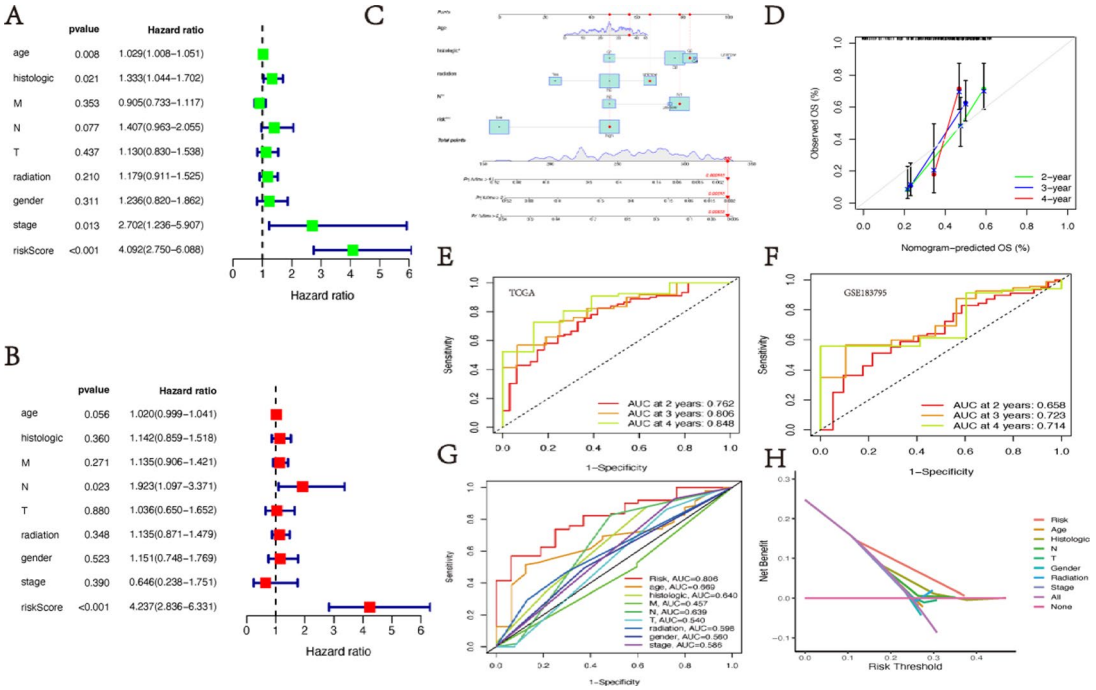


Fig. 7. Construction and evaluation of nomogram. (**A**) Univariate survival analysis of clinicopathological parameters and risk score. (**B**) Multivariate survival analysis of clinicopathological parameters and risk score. (**C**) The possibility of 2-, 3- and 4-year OS was predicted by risk score and clinical characteristics. (**D**) Calibration curves. (**E**-**F**) The ROC curve of the training and validation cohort, respectively. (**G**) 3-year ROC curve of risk score and clinicopathological parameters. (**H**) DCA curve of risk score and clinical characteristics.

was positively correlated with the risk score (Figure.9 A). These observations are basically consistent with the results of the previous cluster analysis. This means that the results obtained from the analysis of high and low risk groups are convincing to a certain extent. Furthermore, we analyzed the correlation between risk ARGs and immune cells (Figure.9B). Additionally, the expression levels of immunosuppressive molecule genes, MHC molecular genes, immune checkpoints and stimulating genes related to antigen presentation and immune response were also different in Figure.9 C-9 F. Most of the genes in several gene clusters showed a high level of expression in high-risk cohorts. This shows that there may be potential distinction in immune status between the distinct groups obtained by individual risk scores.

DNA methylation analysis

Generally, methylation modification of genes can reduce the transcriptional expression of genes. To reveal the correlation between 13 ARPGs and the degree of methylation of its methylation sites and clinical traits (age at initial pathologic diagnosis; histological type; gender; tumor stage simplified; sample type; os event; os), MEXPRESS web server was used to retrieve methylation data for 13 ARPGs in the TCGA PAAD cohort. As a result, we found that age at diagnosis of PAAD showed a weak positive correlation with EIF4EBP1 expression (Spearman, $r=0.173$, $P<0.05$) and PTK6 (Spearman, $r=0.173$, $P<0.05$). Genes significantly negatively correlated with patient survival time are EIF4EBP1 (Spearman, $r=-0.204$, $P<0.01$), CASP4 (Spearman, $r=-0.384$, $P<0.001$), TNFSF10 (Spearman, $r=-0.373$, $P<0.001$), BIRC5 (Spearman, $r=-0.249$, $P<0.001$), PTK6 (Spearman, $r=-0.316$, $P<0.001$), ITGA3 (Spearman, $r=-0.229$, $P<0.01$), BAG3 (Spearman, $r=-0.251$, $P<0.001$), BCL2L1 (Spearman, $r=-0.170$, $P<0.05$), BAK1 (Spearman, $r=-0.274$, $P<0.001$), This result suggests that high expression of these genes may be a driving factor in cancer progression. While GABARAP (Spearman, $r=0.253$, $P<0.001$) and HDAC6 (Spearman, $r=0.203$, $P<0.01$) were significantly positively correlated with patient survival time (Fig. 10).

In addition, the expression of 13 ARPGs were positively correlated with their copy number. The figure.10 shows the relationship between 13 ARPGs and their DNA methylation at different CpG sites.

Copy number variations and genetic mutation

Most CNV are closely related to complex diseases. If CNV occurs in or around the sequence of tumor-related genes, it may cause oncogene activation, tumor suppressor gene inactivation, and eventually lead to tumorigenesis. Additionally, we also studied the mutational status of 28 ARGs in TCGA samples. ULK1 and STK11 deletions were the most common (Figure.11 A). A circos diagram is drawn to show the changes of these regulatory factors characterized by CNV on chromosomes (Figure.11B). And Considering the potential value of somatic mutation in pancreatic carcinoma progression and individualized clinical treatment. Therefore, we analyzed the somatic mutations in pancreatic cancer samples, including the whole group (Figure.11 C) and two distinct risk cohorts

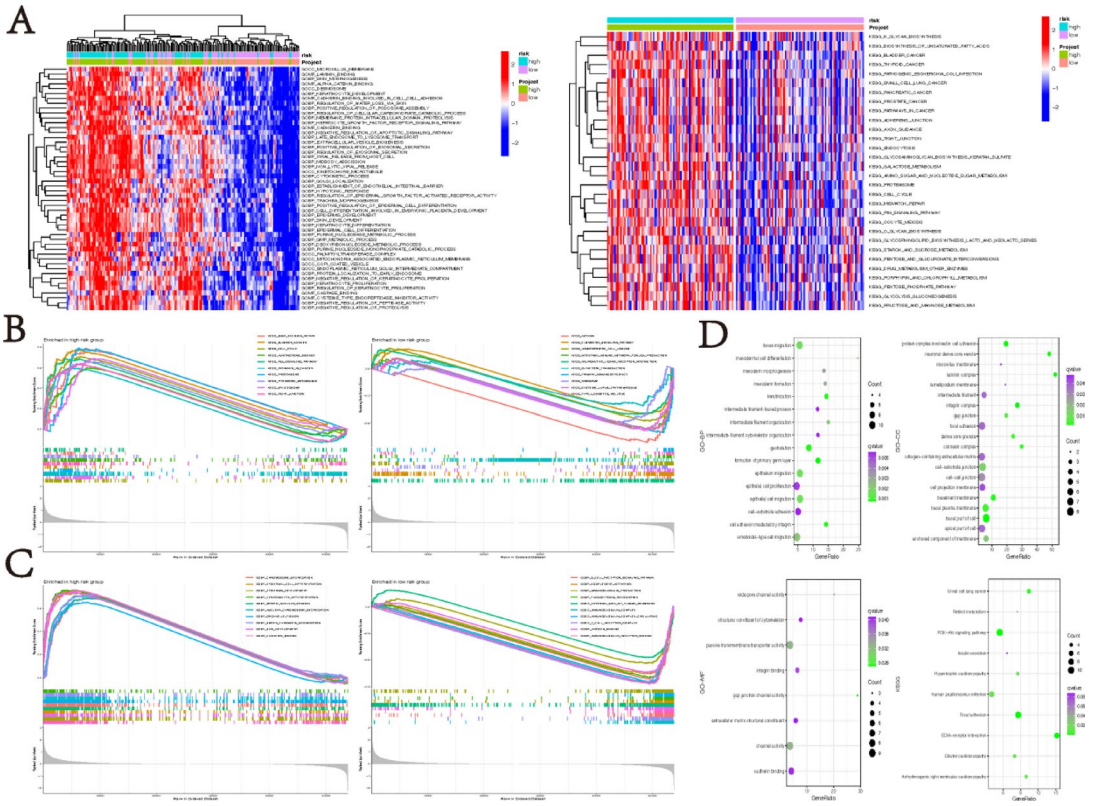


Fig. 8. Biological processes and functional pathways between different risk groups in TCGA-PAAD set. (**A**) Based on GSVA algorithm, GO results (left) and KEGG results (right) between high and low risk groups. (**B**) Based on the GSEA algorithm, show the high risk group (left) and low risk group (right) of the KEGG enrichment pathway. (**C**) GO function annotation based on GSEA algorithm. (**D**) Bubble plots of KEGG pathway and Gene Ontology functional annotation of DEGs between high and low risk groups.

(Figure.11D), and drew the corresponding waterfall plots. Specifically, the mutation frequency of high-risk group was higher than that of low-risk group, and missense mutation was the most common form of mutation in the two distinct risk cohorts. Incidentally, KRAS and TP53 missense mutations were most common in high-risk PC patients, while CDKN2A frameshift deletion was more frequent in low-risk group. Additionally, The relationship between risk score and TMB is discussed. And there is a significant positive correlation between the two variables ($R = 0.3$ $p = 8.1e\text{-}5$), and the TMB score of high-risk patients is higher (Figure.11E-11 F). Low TMB is a favorable prognostic factor[22]. This study found that the OS of pancreatic cancer sufferers with high mutation was worse than that of people with low mutation ($p = 0.009$) (Figure.11G). Among them, the sufferers with high mutation and high risk of pancreatic cancer have the worst prognosis (Figure.11 H).

Drug-Sensitive and cancer stem cell correlation analysis

Through the comprehensive analysis of hundreds of different tumor expression profiles, TIDE algorithm finds biomarkers to predict the efficacy of immune checkpoint inhibitors. Meanwhile, TIDE algorithm is used to evaluate the possibility of immune escape, and finally predict the response of immunotherapy[23]. Therefore, the relationship between risk score and tide score was studied to explore the potential significance of risk model in immunotherapy prediction. Specifically, there was a significant negative correlation between the two distinct risk groups ($R = -0.26$, $p = 5.2e\text{-}4$). High-risk cohorts had lower TIDE scores, suggesting that our risk characteristics have the ability to predict immunotherapy. Low-risk cohorts may be more likely to receive immunotherapy than high-risk cohorts (Figure.12 A). Additionally, we further analyzed the differences of IC50 values of commonly used chemotherapeutic drugs among different risk groups in order to explore feasible sensitive drugs. As shown in Figure.12B, lower IC50 values of AKT inhibitors such as VIII, bicalutamide, CMK, dasatinib, GNF.2, rapatinib, paclitaxel, PD.0325901 and thapsigargin were observed in the high-risk cohort, which means that high-risk sufferers may benefit from these chemotherapeutic drugs. Moreover, low-risk sufferers may benefit from the following drugs, such as Axitinib, Lenalidomide, metformin, Nutlin.3a, Vorinostat. Finally, we analyzed the correlation between risk score and RNAss. The results showed that there was a positive correlation between them. Patients with high risk scores have relatively strong stemness characteristics of tumor cells, so the prognosis is worse than that with low risk scores (Figure.12 C).

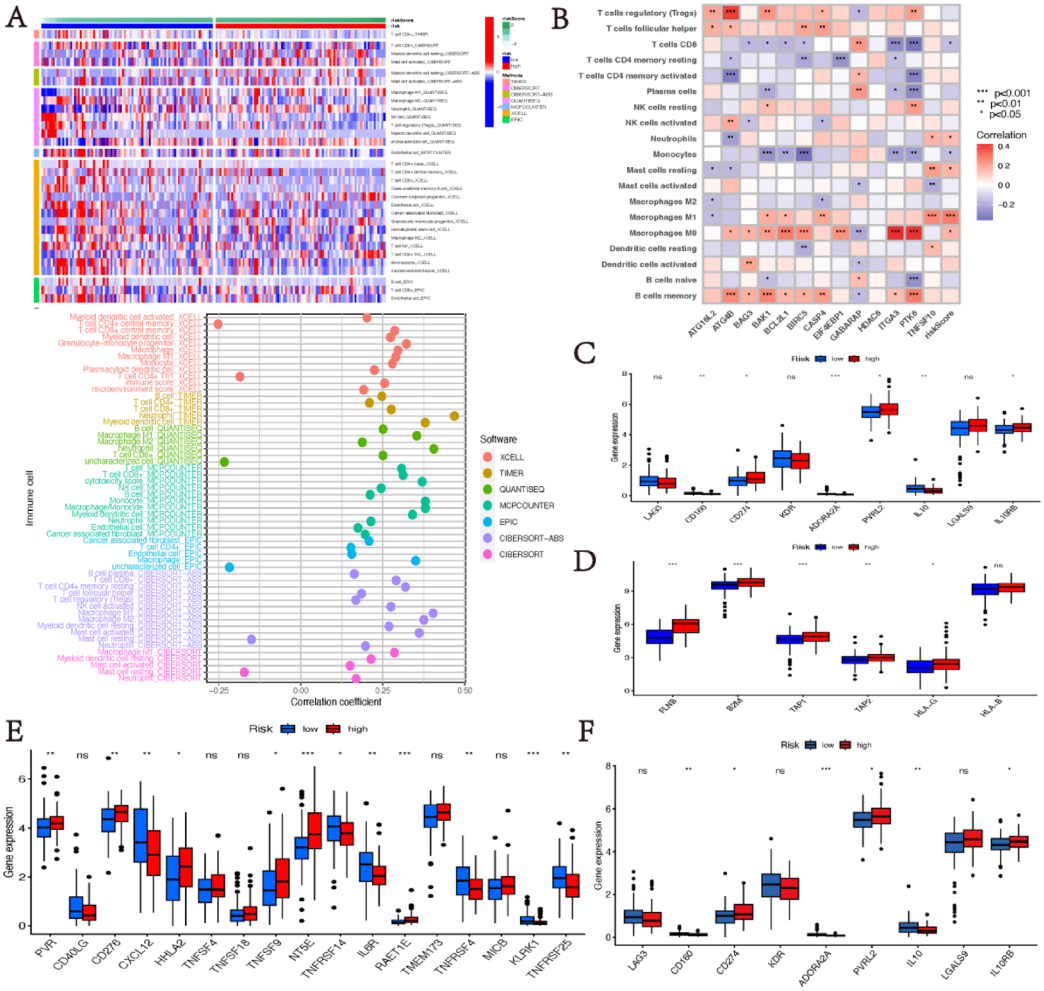


Fig. 9. Immune characteristics of the TCGA-PAAD cohort. (**A**) Heatmap (up) and lollipop plot (down) of differences in infiltrating immunocytes among different risk cohorts. (**B**) Correlation between 13 ARGs and risk scores and infiltrating immune cells. (**C**-**F**) Boxplots of the differences in the expression of Immunosuppressive molecule, MHC molecular, immune checkpoint and stimulator genes among different cohorts. (*$p < 0.05$; **$p < 0.01$; ***$p < 0.001$).

Discussion

Pancreatic carcinoma is one of the most common malignant tumors and has become the second leading cause of cancer-related death[24]. Although various treatments are used in patients with PC, such as surgical resection, chemotherapy, radiotherapy, the 5-year OS rate is still less than 5%[25]. Previous studies have shown that the high mortality rate in patients with pancreatic carcinoma is mainly due to difficult early diagnosis, strong invasiveness and early metastasis[26]. Therefore, it is very important to find new PC biomarkers and understand PC potential mechanism of action. It is also another valuable method to improve the prognosis of PC.

RNA-seq biotechnology can study gene function and gene structure at the overall level, and reveal the molecular mechanism of specific biological processes and disease occurrence. Therefore, it can be used to study the recurrence and metastasis of PAAD[27]. At present, many predictive models were based on unexplored genes, which makes it difficult for doctors to analyze the specific functions of these genes in prognostic markers. And it may not be possible to identify potential targets obtained from markers for personalized treatment development[28]. In this study, we focued on analyzing the prognostic of PAAD and ARGs, constructing nomogram and verifying the accuracy, and deeply understand the relationship between autophagy and PAAD from the aspects of enrichment function, immune cell infiltration, mutation, drug sensitivity and so on.

Previous research have found that ARGs play an important role in many malignant tumors. More specifically, Li and others. (2021) through the analysis of TCGA database, it is proved that 11-autophagy-related lncRNA signal can potentially predict the prognosis of breast cancer[29]. Similarly, Wang et al. screened ARGs related to Glioblastoma by TCGA. The risk score model constructed by NRG1, ITGA3 and MAP1LC3A genes has good predictive ability[30]. Yang et al. (2020) constructed a model of six ARGs to predict the OS of head and neck squamous cancer[31]. Additionally, Zhu et al. divided the sufferers with lung cancer in GEO database into different risk cohorts based on the expression levels of EIF4EBP1, TP63, BNIP3, ATIC, ERO1A and FADD[32]. Similar to our research, a study by Zhou et al. (2021) found that four ARGs (including ATG16L2, GNAI3, APOL1, PTK6)



Fig. 10. DNA methylation analysis of 13 ARPGs. (**A**) EIF4ENP1. (**B**) CASP4. (**C**) GABARAP. (**D**) TNFSF10. (**E**) BIRC5. (**F**) PTK6. (**G**) ITGA3. (**H**) BAG3. (**I**) BCL2L1. (**J**) ATG16L2. (**K**) ATG4B. (**L**) BAK1. (**M**) HDAC6.

were closely related to the prognosis of PAAD, but the analysis was relatively simple[33]. Therefore, we analyzed the biological function and potential molecular mechanism of pancreatic cancer more comprehensively, focusing on the relationship between pancreatic cancer and immune infiltration.

In this study, we collected 28 ARPGs and divided pancreatic cancer samples into two subtypes based on unsupervised cluster analysis. Subsequently, 13 significant ARPGs (including ATG16L2, ATG4B, BAG3, BAK1, BCL2L1, BIRC5, CASP4, EIF4EBP1, GABARAP, HDAC6, ITGA3, PTK6 and TNFSF10) were obtained by univariate COX and LASSO analysis. These genes were used to construct a prognostic model. Their potential relationship with PC, briefly speaking, ATG16L2 is known to be a significant regulator of autophagy and plays an important role in autophagy pathway and tumor development[34]. Additionally, another research on the response of cells to cisplatin used ATG16L2 antibodies to monitor the expression of genes associated with autophagy and cell death. The results showed that cisplatin decreased the level of ATG16L2, suggesting that cisplatin may be a biomarker of platinum resistance in cancer cells[35].

Autophagy-related 4 (ATG4) is the sole cysteine protease[36]. Liu et al. found that targeting ATG4B in various cancer cells may inhibit autophagy and trigger LKB1-AMPK energy sensing pathway, thus inhibiting tumor growth[37]. Studies have shown that pancreatic carcinoma cells are easily inhibited by ATG4B. This is most common in PC that depend on mutant K-RAS expression[38]. Some scholars have proposed a model of how autophagy promotes PC growth, such as the ability to provide metabolites and tumor response to stress[39]. Recently, it had been found that ribose-5-phosphate isomerase (autophagy-related enzymes) participates in drug resistance of KRAS-dependent PC by regulating nucleotide synthesis[40,41]. The inhibition of autophagy of KRAS-dependent PC is also an important reason for DNA damage and increased apoptosis. It is also found that autophagy limits DNA damage stress in PC, which may be affected by p53 status[42,43]. Similarly, autophagy inhibition may also affect the surrounding stromal cells[44,45]. This coincides with the fact that our study found that high-risk groups are associated with multiple metabolic pathways.

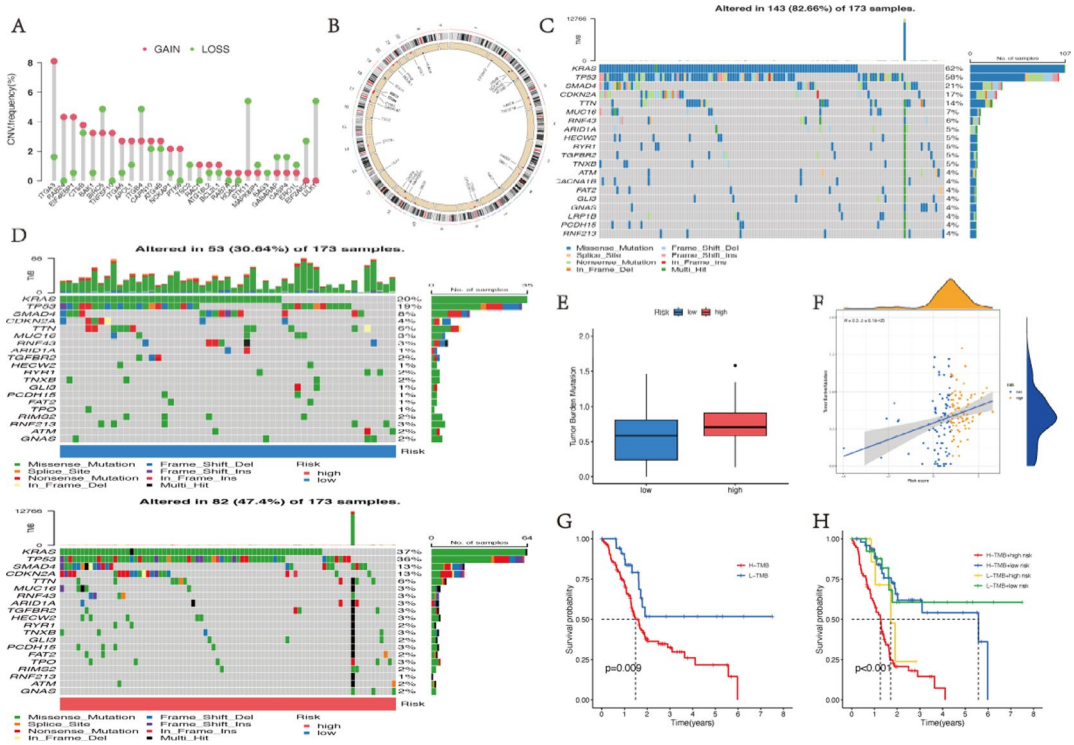


Fig. 11. Copy number variation and gene mutation in pancreatic cancer. (**A**) Copy number variation frequency of ARGs. (**B**) CNV location of ARGs on chromosomes. (**C**) All the gene mutations in the TCGA-PAAD queue and show the top 20 genes shown in the waterfall plot. (D) The waterfall plots shows the characteristics of gene mutations in the low- cohort (top) and the high-risk cohort (bottom). (**E**) The boxplot of TMB score difference between different risk cohorts. (**F**) the linear relationship between risk score and TMB score. (**G**) The KM curve of the OS of distinct TMB groups and (**H**) the combination of TMB and risk score.

BAG3 is a multi-domain protein that plays an important role in a variety of cellular processes, such as the control of apoptosis, autophagy[46,47]. Recently, some scholars have found that BAG3 can be secreted by pancreatic cancer cells and other tumor cells. Secreted BAG3 can stimulate tumor interstitial macrophages to release factors that maintain cancer growth and metastasis. Meanwhile, BAG3 neutralization has the potential to treat PC[48]. And BAG3 is an important anti-apoptosis protein[49,50]. The damage of apoptosis or the increase of anti-apoptotic proteins may affect the progression of tumor. Some scholars have found that miR-340 can negatively regulate BAG3 and inactivate PI3K/AKT pathway. The deficiency of PI3K/AKT signal pathway increases the release of cytochrome c and the activity of caspase, which increases the apoptosis of cells[51,52].

BAK1 can promote apoptosis[53]. Studies have shown that itraconazole inhibits the proliferation of PC cells by activating the mechanism of apoptosis induced by Bak-1[54]. GABARAP is thought to be down-regulated in malignant tumors, while high expression is associated with a good prognosis[55]. Activation of RAS signal transduction pathway exists in about 30% of human cancers. GABARAP is associated with carcinogenic KRAS mutations and poor prognosis of PC. This indicates the potential tumor inhibitory effect of this pathway in RAS-driven human tumor[56]. Some studies have shown that GABARAP may inhibit the malignant behavior of breast carcinoma through AKT/mTOR pathway[57].

HDAC is closely related to the occurrence and development of cancer[58]. The immunofluorescence data of Yang et al. show that inhibition of HDAC6 can induce autophagy of PC cells[59]. PC is a highly malignant tumor, which usually involves the deregulation of c-Myc gene. Fu et al. found an anti-tumor mechanism in PC cells: it can down-regulate the level of c-Myc protein by inhibiting HDAC6 subunit[60]. ITGA3 usually interacts with extracellular matrix proteins and plays an important role in cancer metastasis[61]. Hippo pathway effector YAP1 is an effective transcriptional coactivator, which forms a complex with ZEB1 and activates ITGA3 transcription in PC cells through YAP1/transcriptional enhancement related domain binding sites. ZIP4-miR-373-LATS2-ZEB1/YAP1-ITGA3 signal axis has a significant effect on PC metastasis and EMT plasticity[62]. PTK6 is expressed in a variety of malignant tumors, including PC. Studies have shown that PTK6 gene silencing increased cell survival rate and decreased apoptosis after drug therapy, while overexpression of PTK6 decreased cell survival rate and increased apoptosis rate[63]. And it has also been proved that PTK6 regulates the migration and invasion of PC cells through ERK signal transduction[64].

TNFSF10 (also known as TRAIL) is a cytokine that can selectively induce apoptosis of tumor cells without causing damage to normal cells, which is promising in tumor therapy. At the same time, resistance to TRAIL-induced apoptosis has been found in many primary cacner and tumor cell lines, including many human PC cell lines[65]. Specifically, Ozawa et al. found that the expression levels of TRAIL, DR4 and DR5 in PC tissues were

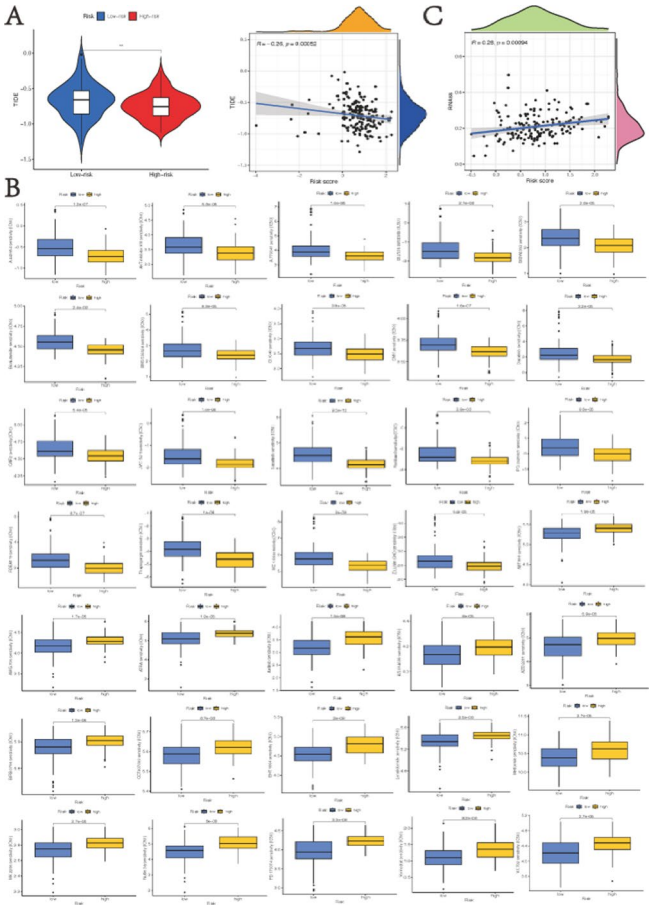


Fig. 12. Cancer Stem Cell Correlation and drug sensitivity analyses of PC patients with two distinct risk scores. (**A**) Violin plot of TIDE scores differences among different risk cohorts (left) and their linear correlation (right). (**B**) Prediction of chemosensitivity between high and low risk cohorts. (**C**) The correlation between risk score and RNAss.

significantly higher than those in normal tissues. Some scholars have found that overexpression of MUC5AC in human PC can inhibit TRAIL-induced apoptosis of human PC cells, thus promoting tumor growth and metastasis[66–69]. EIF4EBP1 encodes a translation inhibitory protein[70,71]. This protein is the main substrate of mTOR and plays an important role in mTOR signaling pathway[72]. Promote cell growth and proliferation by responding to activated mTOR signaling pathways[73]. EIF4EBP1 is involved in the development and progressionof cancer and is associated with poor survival of cancer persons[74]. EIF4EBP1 promotes tumor adaptation to metabolic and genotoxic stress by selectively enhancing or blocking the translation of specific transcripts[75,76]. Some scholars have found that inhibiting the expression of mTOR/EIF4EBP1 axis can effectively inhibit the growth of PC tumor[77].

In addition, the research on the role of residual risk genes (including BIRC5, CASP4 and BCL2L1) in PC is still insufficient, and their potential functions need to be further studied.

After constructing the risk signature related to autophagy, we further explore its significance in PC from many aspects of biology. In addition, PC persons were divided into two distinct risk groups based on the median risk score, and the prognosis of high-risk person is worse than that of low-risk person. Combined with the clinicopathological parameters, the nomogram was constructed. ROC curve and calibration curves prove the accuracy and specificity of the model, and verified by the independent PC cohort of GEO, indicating that our risk profile is stable and reliable. Subsequently, we also discussed the relationship between risk score and clinical characteristics, and the results showed that patients with high risk score usually had poor clinicopathological features. In addition, the enrichment analysis results of GSEA and GSVA also revealed the biological function of patients in different risk cohorts and different clusters. Furthermore, the difference of immune microenvironment composition in PC was analyzed by ssGSEA and CIBERSORT algorithms. The above comprehensive analysis of pancreatic cancer is helpful to further explore the goal of intervention and guide individualized treatment strategies.

Conclusion

In brief, this study reveals a new risk signal associated with autophagy, which can be used to evaluate the prognosis of PC persons. Although a variety of methods have been used to evaluate our model, there are still some

limitations. In addition, our study has no experimental verification, so there are serious limitations. The model is still promising. In the future, pancreatic cancer tissue can be collected by surgery, then immunofluorescence staining and Western blotting can be performed to verify the predictive ability of the model[78]. Similarly, we can collect clinicopathological parameters to further analyze the significance of ARGs in PC therapy. In summary, we constructed a patient stratified model consisting of 13 ARGs. This model can effectively distinguish PC persons and play an important role in the accurate therapy of PC persons in the future.

Data availability

The datasets analysed during the current study are available in the TCGA database (TCGA-PAAD) and GEO database (GSE183795). Further inquiries can be directed to the corresponding author.

Received: 22 April 2025; Accepted: 28 October 2025
Published online: 26 November 2025

References

1. Mizrahi, J. D. et al. *Shroff Pancreat. Cancer Lancet*, **395** (10242) 2008–2020. (2020).
2. Rahib, L. et al. Projecting cancer incidence and deaths to 2030: the unexpected burden of thyroid, liver, and pancreas cancers in the united States. *Cancer Res.* **74** (11), 2913–2921 (2014).
3. Kamisawa, T. et al. Pancreatic cancer. *Lancet* **388** (10039), 73–85 (2016).
4. Neoptolemos, J. P. et al. Therapeutic developments in pancreatic cancer: current and future perspectives. *Nat. Reviews Gastroenterol. Hepatol.* **15** (6), 333–348 (2018).
5. Klionsky, D. J., Petroni, G. & Amaravadi, R. K. Autophagy in major human diseases. *EMBO J.* **40** (19), e108863. https://doi.org/10.15252/embj.2021108863 (2021). Epub 2021 Aug 30. PMID: 34459017; PMCID: PMC8488577.
6. Cassidy, L. D. et al. Temporal Inhibition of autophagy reveals segmental reversal of ageing with increased cancer risk. *Nat. Commun.* **11**, 307 (2020).
7. Yamamoto, K. et al. Autophagy promotes immune evasion of pancreatic cancer by degrading MHC-I. *Nature* **581**, 100–105 (2020).
8. Kaludercic, N. et al. Comprehensive autophagy evaluation in cardiac disease models. *Cardiovasc. Res.* **116**, 483–504 (2020).
9. Rubinsztein, D. C., Bento, C. F. & Deretic, V. Therapeutic targeting of autophagy in neurodegenerative and infectious diseases. *J. Exp. Med.* **212**, 979–990 (2015).
10. Menikdiwela, K. R. et al. Autophagy in metabolic syndrome: breaking the wheel by targeting the renin-angiotensin system. *Cell. Death Dis.* **11**, 87 (2020).
11. Zeng, Z. et al. MicroRNA-21 aggravates chronic obstructive pulmonary disease by promoting autophagy. *Exp. Lung Res.* **44**, 89–97 (2018).
12. Choi, M. E. Autophagy in kidney disease. *Annu. Rev. Physiol.* **82**, 297–322 (2020).
13. Keller, M. D., Torres, V. J. & Cadwell, K. Autophagy and microbial pathogenesis. *Cell. Death Differ.* **27**, 872–886 (2020b).
14. Yin, X. et al. Autophagy in bone homeostasis and the onset of osteoporosis. *Bone Res.* **7**, 28 (2019).
15. Onorati, A. V. et al. Targeting autophagy in cancer. *Cancer* **124** (16), 3307–3318. https://doi.org/10.1002/cncr.31335 (2018).
16. Li, X., He, S. & Ma, B. Autophagy and autophagy-related proteins in cancer. *Mol. Cancer*. **19** (1), 12. https://doi.org/10.1186/s12943-020-1138-4 (2020). PMID: 31969156; PMCID: PMC6975070.
17. Sui, X. et al. Autophagy and chemotherapy resistance: a promising therapeutic target for cancer treatment. *Cell. Death Dis.* **4**, e838. https://doi.org/10.1038/cddis.2013.350 (2013).
18. Yamazaki, T. et al. Mitochondrial DNA drives abscopal responses to radiation that are inhibited by autophagy. *Nat. Immunol.* **21**, 1160–1171 (2020).
19. Poillet-Perez, L. et al. Autophagy maintains tumour growth through Circulating arginine. *Nature* **563**, 569–573 (2018).
20. Ying, B., Xu, W., Nie, Y. & Li, Y. HSPA8 is a new biomarker of triple negative breast cancer related to prognosis and immune infiltration. *Dis. Markers*. **2022**, 8446857 (2022).
21. Kanehisa, M., Furumichi, M., Sato, Y., Matsuura, Y. & Ishiguro-Watanabe, M. KEGG: biological systems database as a model of the real world. *Nucleic Acids Res.* **53**, D672–D677 (2025).
22. Liu, L., Bai, X. & Wang, J. Combination of TMB and CNA stratifies prognostic and predictive responses to immunotherapy across metastatic cancer. *Clin. Cancer Res.* **25** (24), 7413–7423 (2019).
23. Wu, Z. H. & Yang, D. L. Epigenetic and immune-cell infiltration changes in the tumor microenvironment in hepatocellular carcinoma. *Front. Immunol.* **12**, 793343 (2021).
24. Anuradha, R. et al. Pancreatic cancer biology and genetics from an evolutionary perspective. *Nat. Rev. Cancer*. **16**, 553–565 (2016).
25. Bapat, A. A., Hostetter, G., Von Hoff, D. D. & Han, H. Perineural invasion and associated pain in pancreatic cancer. *Nat. Rev. Cancer*. **11**, 695–707 (2011).
26. Jin, H., Wu, Y. & Tan, X. The role of pancreatic cancer-derived exosomes in cancer progress and their potential application as biomarkers. *Clin. Translational Oncology:official Publication Federation Span. Oncol. Soc. Natl. Cancer Inst. Mexico*. **19**, 921–930 (2017).
27. Cao, L., Huang, C. & Cui Zhou, D. Proteogenomic characterization of pancreatic ductal adenocarcinoma. *Cell* **184** (19), 5031–5052e26. https://doi.org/10.1016/j.cell.2021.08.023 (2021).
28. Xie, Y. et al. A Necroptosis-Related gene signature to predict the prognosis of skin cutaneous melanoma. *Dis. Markers*. **2022**, 8232024. https://doi.org/10.1155/2022/8232024 (2022). PMID: 36438905; PMCID: PMC9683951.
29. Li, X., Jin, F. & Li, Y. A novel autophagy-related LncRNA prognostic risk model for breast cancer. *J. Cell. Mol. Med.* **25** (1), 4–14. https://doi.org/10.1111/jcmm.15980 (2021). Epub 2020 Nov 20. PMID: 33216456; PMCID: PMC7810925.
30. Wang, Z., Gao, L. & Guo, X. Development and validation of a nomogram with an autophagy-related gene signature for predicting survival in patients with glioblastoma. *Aging (Albany NY)*. **11** (24), 12246–12269. https://doi.org/10.18632/aging.102566 (2019). Epub 2019 Dec 17. PMID: 31844032; PMCID: PMC6949068.
31. Yang, C. et al. Prognostic correlation of an Autophagy-Related gene signature in patients with head and neck squamous cell carcinoma. *Comput. Math. Methods Med.* **2020**, 7397132. https://doi.org/10.1155/2020/7397132 (2020). PMID: 33456497; PMCID: PMC7785385.
32. Zhu, J., Wang, M. & Hu, D. Development of an autophagy-related gene prognostic signature in lung adenocarcinoma and lung squamous cell carcinoma. *PeerJ* **8**, e8288. https://doi.org/10.7717/peerj.8288 (2020). PMID: 31938577; PMCID: PMC6953332.
33. Zhou, Q. et al. A Four Autophagy-Related Gene-Based Prognostic Signature for Pancreatic Cancer. Crit Rev Eukaryot Gene Expr. **31**(4):89–100. (2021). https://doi.org/10.1615/CritRevEukaryotGeneExpr.2021038733. PMID: 34587439.
34. Ishibashi, K. et al. Atg16L2, a novel isoform of mammalian Atg16L that is not essential for canonical autophagy despite forming an Atg12-5-16L2 complex. *Autophagy* **7**, 1500–1513 (2011).
35. Huang, Y., Chuang, A. Y. & Ratovitski, E. A. Phospho-DeltaNp63alpha/miR-885–3p axis in tumor cell life and cell death upon cisplatin exposure. *Cell. Cycle*. **10**, 3938–3947 (2011).

36. Park, N. Y., Jo, D. S. & Cho, D. H. Post-Translational modifications of ATG4B in the regulation of autophagy. *Cells* **11** (8), 1330. https://doi.org/10.3390/cells11081330 (2022).
37. Liu, P. F. et al. Ablation of ATG4B suppressed autophagy and activated AMPK for cell cycle arrest in cancer cells. *Cell. Physiol. Biochem.* **44** (2), 728–740. https://doi.org/10.1159/000485286 (2017).
38. Seo, J. W. et al. Autophagy is required for PDAC glutamine metabolism. *Sci. Rep.* **6**, 37594. https://doi.org/10.1038/srep37594 (2016).
39. Viale, A. et al. Oncogene ablation-resistant pancreatic cancer cells depend on mitochondrial function. *Nature* **514**, 628–632. https://doi.org/10.1038/nature13611 (2014).
40. Heintze, J. et al. Ribose 5-phosphate isomerase inhibits LC3 processing and basal autophagy. *Cell. Signal.* **28**, 1380–1388. https://doi.org/10.1016/j.cellsig.2016.06.015 (2016).
41. Santana-Codina, N. et al. Oncogenic KRAS supports pancreatic cancer through regulation of nucleotide synthesis. *Nat. Commun.* **9**, 4945. https://doi.org/10.1038/s41467-018-07472-8 (2018).
42. Yang, A. & Kimmelman, A. C. Inhibition of autophagy attenuates pancreatic cancer growth independent of TP53/TRP53 status. *Autophagy* **10**, 1683–1684. https://doi.org/10.4161/auto.29961 (2014).
43. Rosenfeldt, M. T. et al. p53 status determines the role of autophagy in pancreatic tumour development. *Nature* **504**, 296–300. https://doi.org/10.1038/nature12865 (2013).
44. Sousa, C. M. et al. Pancreatic stellate cells support tumour metabolism through autophagic Alanine secretion. *Nature* **536**, 479–483. https://doi.org/10.1038/nature19084 (2016).
45. Agrotis, A. & Ketteler, R. On ATG4B as drug target for treatment of solid Tumours-The knowns and the unknowns. *Cells* **9** (1), 53. https://doi.org/10.3390/cells9010053 (2019). PMID: 31878323; PMCID: PMC7016753.
46. De Marco, M. et al. An emerging role for BAG3 in gynaecological malignancies. *Br. J. Cancer*. **125** (6), 789–797. https://doi.org/10.1038/s41416-021-01446-2 (2021). Epub 2021 Jun 7. PMID: 34099896; PMCID: PMC8437940.
47. Deng, J. et al. Identification of an autophagy-related gene signature for predicting prognosis and immune activity in pancreatic adenocarcinoma. *Sci. Rep.* **12**, 7006 (2022).
48. De Marco, M. et al. Role of BAG3 in cancer progression: A therapeutic opportunity. *Semin Cell. Dev. Biol.* **78**, 85–92. https://doi.org/10.1016/j.semcdb.2017.08.049 (2018). Epub 2017 Aug 31. PMID: 28864347.
49. Kogel, D. et al. At the crossroads of apoptosis and autophagy: multiple roles of the co-chaperone BAG3 in stress and therapy resistance of cancer. *Cells* **9**, 574 (2020).
50. Marzullo, L., Turco, M. C. & De Marco, M. The multiple activities of BAG3 protein: mechanisms. *Biochim. Biophys. Acta Gen. Subj.* **1864**, 129628 (2020).
51. Singh, M. V. et al. MicroRNA regulation of BAG3. *Exp. Biol. Med. (Maywood)*. **247** (8), 617–623 (2022). doi: 10.1177/15353702211066908. Epub 2022 Jan 15. PMID: 35037515; PMCID: PMC9039493.
52. Liu, J. et al. MiR-143 enhances the antitumor activity of Shikonin by targeting BAG3 expression in human glioblastoma stem cells. *Biochem. Biophys. Res. Commun.* **468**, 105–112 (2015).
53. Qin, J. et al. Association between BAK1 gene rs210138 polymorphisms and testicular germ cell tumors: A systematic review and Meta-Analysis. *Front. Endocrinol. (Lausanne)*. **11**, 2 (2020). PMID: 32038496; PMCID: PMC6989409.
54. Strasser, A. & Vaux, D. L. Viewing BCL2 and cell death control from an evolutionary perspective. *Cell. Death Differ.* **25** (1), 13–20. https://doi.org/10.1038/cdd.2017.145 (2018). Epub 2017 Nov 3. PMID: 29099481; PMCID: PMC5729521.
55. Jacquet, M. et al. The functions of Atg8-family proteins in autophagy and cancer: linked or unrelated? Autophagy. **17**(3):599–611. (2021). https://doi.org/10.1080/15548627.2020.1749367. Epub 2020 Apr 19. PMID: 32255730; PMCID: PMC8032235.
56. Manent, J. et al. Autophagy suppresses Ras-driven epithelial tumourigenesis by limiting the accumulation of reactive oxygen species. Oncogene. **36**(40):5576–5592. (2017). https://doi.org/10.1038/onc.2017.175. Epub 2017 Jun 5. Erratum in: Oncogene. 2017;36(40):5658–5660. PMID: 28581519; PMCID: PMC5633656.
57. Liu, Y. et al. GABARAP suppresses EMT and breast cancer progression via the AKT/mTOR signaling pathway. *Aging (Albany NY)*. **13** (4), 5858–5874. https://doi.org/10.18632/aging.202510 (2021). Epub 2021 Feb 11. PMID: 33591943; PMCID: PMC7950252.
58. Gaisina, I. N. et al. Identification of HDAC6-Selective inhibitors of low cancer cell cytotoxicity. *ChemMedChem* **11** (1), 81–92. https://doi.org/10.1002/cmdc.201500456 (2016). Epub 2015 Nov 23. PMID: 26592932; PMCID: PMC4818591.
59. Yang, Y. et al. MicroRNA-221 induces autophagy through suppressing HDAC6 expression and promoting apoptosis in pancreatic cancer. *Oncol. Lett.* **16** (6), 7295–7301. https://doi.org/10.3892/ol.2018.9513 (2018). Epub 2018 Sep 27. PMID: 30546469; PMCID: PMC6256293.
60. Fu, X. H. et al. CUDC-907 displays potent antitumor activity against human pancreatic adenocarcinoma in vitro and in vivo through Inhibition of HDAC6 to downregulate c-Myc expression. *Acta Pharmacol. Sin.* **40** (5), 677–688. https://doi.org/10.1038/s41401-018-0108-5 (2019). Epub 2018 Sep 17. PMID: 30224636; PMCID: PMC6786396.
61. Jiao, Y. et al. ITGA3 serves as a diagnostic and prognostic biomarker for pancreatic cancer. *Onco Targets Ther.* **12**, 4141–4152 (2019). PMID: 31213833; PMCID: PMC6549486.
62. Liu, M. et al. Zinc-Dependent regulation of ZEB1 and YAP1 coactivation promotes Epithelial-Mesenchymal transition plasticity and metastasis in pancreatic cancer. *Gastroenterology* **160** (5), 1771–1783e1. https://doi.org/10.1053/j.gastro.2020.12.077 (2021). Epub 2021 Jan 6. PMID: 33421513; PMCID: PMC8035249.
63. Ono, H., Basson, M. D. & Ito, H. PTK6 potentiates Gemcitabine-Induced apoptosis by prolonging S-phase and enhancing DNA damage in pancreatic cancer. *Mol. Cancer Res.* **13** (8), 1174–1184. https://doi.org/10.1158/1541-7786.MCR-15-0034 (2015). Epub 2015 May 26. PMID: 26013168.
64. Ono, H., Basson, M. D. & Ito, H. PTK6 promotes cancer migration and invasion in pancreatic cancer cells dependent on ERK signaling. *PLoS One*. **9** (5), e96060. https://doi.org/10.1371/journal.pone.0096060 (2014). PMID: 24788754; PMCID: PMC4006869.
65. Nahacka, Z. et al. TRAIL induces apoptosis but not necroptosis in colorectal and pancreatic cancer cells preferentially via the TRAIL-R2/DR5 receptor. *Biochim. Biophys. Acta Mol. Cell. Res.* **1865** (3), 522–531 (2018). Epub 2017 Dec 24. PMID: 29278689.
66. Huang, M. et al. A novel TRAIL mutant-TRAIL-Mu3 enhances the antitumor effects by the increased affinity and the up-expression of DR5 in pancreatic cancer. *Cancer Chemother. Pharmacol.* **82** (5), 829–838. https://doi.org/10.1007/s00280-018-3658-9 (2018). Epub 2018 Aug 24. PMID: 30167846.
67. Ozawa, F. et al. Effects and expression of TRAIL and its apoptosis-promoting receptors in human pancreatic cancer. Cancer Lett. **163**(1):71–81. (2001). https://doi.org/10.1016/s0304-3835(00)00660-1. PMID: 11163110.
68. Hoshi, H. et al. Tumor-associated MUC5AC stimulates in vivo tumorigenicity of human pancreatic cancer. *Int. J. Oncol.* **38** (3), 619–627. https://doi.org/10.3892/ijo.2011.911 (2011). Epub 2011 Jan 18. PMID: 21249315.
69. Hoshi, H. et al. MUC5AC protects pancreatic cancer cells from TRAIL-induced death pathways. Int J Oncol. **42**(3):887 – 93. (2013). https://doi.org/10.3892/ijo.2013.1760. Epub 2013 Jan 3. PMID: 23292004.
70. Harris, T. E. & Lawrence, J. C. Jr. TOR signaling. Sci STKE 2003: re15. pmid:14668532. (2003).
71. Gingras, A. C., Raught, B. & Sonenberg, N. eIF4 initiation factors: effectors of mRNA recruitment to ribosomes and regulators of translation. *Annu. Rev. Biochem.* **68**, 913–963 (1999). pmid:10872469.
72. Aoyagi, M., Gaspar, M. & Shenk, T. E. Human cytomegalovirus UL69 protein facilitates translation by associating with the mRNA cap-binding complex and excluding 4EBP1. *Proc. Natl. Acad. Sci. U S A*. **107**, 2640–2645 (2010). pmid:20133758.
73. Thoreen, C. C. Many roads from mTOR to eIF4F. *Biochem. Soc. Trans.* **41**, 913–916 (2013). pmid:23863155.

74. Karlsson, E. et al. The mTOR effectors 4EBP1 and S6K2 are frequently coexpressed, and associated with a poor prognosis and endocrine resistance in breast cancer: a retrospective study including patients from the randomised Stockholm tamoxifen trials. Breast Cancer Res 15: R96. pmid:24131622. (2013).
75. Musa, J., Orth, M. F. & Dallmayer, M. Eukaryotic initiation factor 4E-binding protein 1 (4E-BP1): a master regulator of mRNA translation involved in tumorigenesis. *Oncogene* **35** (36), 4675–4688. https://doi.org/10.1038/onc.2015.515 (2016). Epub 2016 Feb 1. PMID: 26829052.
76. Wan, P. et al. BRDT is a novel regulator of eIF4EBP1 in renal cell carcinoma. *Oncol. Rep.* **44** (6), 2475–2486. https://doi.org/10.3892/or.2020.7796 (2020). Epub 2020 Oct 8. PMID: 33125143; PMCID: PMC7610328.
77. Müller, D., Shin, S. & Goullet de Rugy, T. eIF4A Inhibition circumvents uncontrolled DNA replication mediated by 4E-BP1 loss in pancreatic cancer. *JCI Insight*. **4** (21), e121951. https://doi.org/10.1172/jci.insight.121951 (2019). PMID: 31672935; PMCID: PMC6948775.
78. Zhang M. et al. Five EMT-related genes signature predicts overall survival and immune environment in microsatellite instability-high gastric cancer. *Cancer Med.* **12**(2): 2075–2088. https://doi.org/10.1002/cam4.4975IF, (2023).

Acknowledgements
The authors thank the TCGA project, GEO project and other groups for providing invaluable datasets for statistical analyses.

Author contributions
BCY and XJW designed the study. BCY and XYW conducted the data-mining analyses and wrote the manuscript. BCY, XJW and XYW made the relative clinical statistics and pictures. All the authors have read and approved the manuscript.

Declarations

Competing interests
The authors declare no competing interests.

Notes for publishers
All propositions expressed in the article represent only those of the author, not necessarily those of publishers, editors and reviewers.

Ethical statement
The data utilized in this study were obtained from public access databases: The TCGA and the GEO. All data are de-identified and publicly available for research use. Therefore, this study did not require additional ethical approval from our institutional review board. The acquisition and application of all data in this analysis were conducted in accordance with the ethical guidelines and data use policies specified by TCGA, GEO, and the respective original studies.

Additional information
Supplementary Information The online version contains supplementary material available at https://doi.org/10.1038/s41598-025-26358-6.

Correspondence and requests for materials should be addressed to B.Y.

Reprints and permissions information is available at www.nature.com/reprints.

Publisher's note Springer Nature remains neutral with regard to jurisdictional claims in published maps and institutional affiliations.

Open Access This article is licensed under a Creative Commons Attribution-NonCommercial-NoDerivatives 4.0 International License, which permits any non-commercial use, sharing, distribution and reproduction in any medium or format, as long as you give appropriate credit to the original author(s) and the source, provide a link to the Creative Commons licence, and indicate if you modified the licensed material. You do not have permission under this licence to share adapted material derived from this article or parts of it. The images or other third party material in this article are included in the article's Creative Commons licence, unless indicated otherwise in a credit line to the material. If material is not included in the article's Creative Commons licence and your intended use is not permitted by statutory regulation or exceeds the permitted use, you will need to obtain permission directly from the copyright holder. To view a copy of this licence, visit http://creativecommons.org/licenses/by-nc-nd/4.0/.

© The Author(s) 2025